Optical properties and complex refractive index of Co doped ZnO waveguide thin films elaborated by spray pyrolysis

Halima DJAABOUBE (halimadjaaboube@hotmail.fr)
Constantine 1 university
Abdelouadoud MAMMERI
Constantine 1 university https://orcid.org/0000-0003-3820-3324
Yassine Bouachiba
Constantine 3 university
Adel TAABOUCHE1
Constantine 1 university
Abderrahmane BOUABELLOU
Constantine 1 university
Hacene SERRAR3
3Research Center in Industrial Technologies (CRTI)
Ilyes Sekhri
Ferhat Abbas university
Badis RAHAL
Nuclear Research Center of Algiers

Research Article

Keywords: ZnO, spray pyrolysis, waveguide, refractive index, extinction coefficient, prism coupler, UV-Vis.

Posted Date: April 1st, 2022

DOI: https://doi.org/10.21203/rs.3.rs-1513013/v1

Optical properties and complex refractive index of Co doped ZnO waveguide thin films elaborated by spray pyrolysis

Halima DJAABOUBE *[1], Abdelouadoud MAMMERI[1], Yassine Bouachiba[2], Adel TAABOUCHE[1], Abderrahmane BOUABELLOU[1], Hacene SERRAR[3], Ilyes Sekhri[4], and Badis RAHAL[5]

[1]Laboratoire Couches Minces et Interfaces, Université de Fréres Mentouri Constantine 1, Constantine, Algérie.
[2]Laboratoire Technologie des Matériaux Avancés, Ecole Nationale Polytechnique de Constantine Malek BENNABI,BP 75A RP, Ali Mendjeli, Constantine, Algérie.
[3]Research Center in Industrial Technologies (CRTI), BP 64 Cheraga, Alger, Algeria.
[4]Laboratoire Dosage, Analyse et Caractérisation en Haute Résolution, Université Ferhat Abbas, Sétif, Algérie.
[5]Nuclear Techniques Division, Nuclear Research Center of Algiers, 2 Bd, Frantz Fanon, BP 399, 16000, Algiers, Algeria.

February 2, 2022

*halimadjaaboube@hotmail.fr

Abstract

$Co_xZn_{1-x}O$ (x = 0.00, 0.04, 0.08 and 0.10) thin films were sprayed pyrolysis onto ordinary glass substrates. The micro Raman spectroscopy revealed the presence of wurtzite structure in all films. The UV-Vis investigation showed good optical transmittance in the visible region with the increase in the absorption bands related to internal Co^{+2} d-d transitions over Co concentration. The optical gap energy decreased by 0.34 eV as Co doping increased, contrary to Urbach energy which increased by 230 meV. The SEM observation indicated obvious modification in the morphology of the films. M-lines spectroscopy measured the ordinary refractive index which was found to increase by 0.0156 as the Co doping increased. Cobalt doping provoked the extinction of light coupling and propagation in the films manifested as an increase in full width at the half maximum of the guided peaks and a decrease in the reflected intensity. This was due to the increase in the extinction coefficient measured by UV-Vis spectroscopy.

Keywords: ZnO, spray pyrolysis, waveguide, refractive index, extinction coefficient, prism coupler, UV-Vis.

1 Introduction

The developments of all forms of optical waveguides led to huge development in numerous fields like communications, integrated optics, lasers and photonics. Optical fibers are relatively flexible and immune to electromagnetic interference so they found use in communications. Transparent thin films waveguides are of high quality, controllable and efficient and by that, they had been employed as bio and chemical sensors [1–3], integrated optical amplifier [4] and a guided layer in total internal reflection fluorescence microscope [5] to name a few. A dielectric waveguide can be defined as any structure used to control the flow of electromagnetic waves in a certain direction. This guiding is possible by confining the electromagnetic wave within its surfaces. In order to understand the propagation of light in a waveguide, it is essential to characterize the refractive index and the extinction coefficient of the waveguide as the refractive index is a measure of the phase difference between the source wave and oscillating charges in the media and the extinction coefficient is a direct measure of the attenuation of the wave inside the media [6].

In the last decade, Zinc oxide (ZnO) related research numbers grew largely because of new or improved types of electronic and photonic devices [7]. Waveguide structures based on ZnO have been demonstrated and suggest possible applications of ZnO thin films in opto-electronics and integrated optics [8–11]. For a better understanding and control over ZnO thin film waveguide, it is necessary to perform an accurate and direct characterization of its optical properties including the refractive index. Several techniques of optical characterization of thin films are used such as absorption/transmission

spectroscopy and ellipsometry. The latter can reveal the refractive index, thickness, and extinction coefficient [12]. Prism coupler based method alternatively called m-lines spectroscopy has been developed since the '70s to characterize thin films. It measures the refractive index with 2×10^{-4} accuracy and the thickness with 0.5% [13].

The effect of dopants on the refractive index of ZnO is not very obvious and is still a subject of interest. The root of the optical properties of a semiconductor is intimately related to both intrinsic and extrinsic effects. Intrinsic ones are manifested via the transitions taking place between the electrons and holes in the conduction and in the valence band respectively, in addition to excitonic effects due to the Coulomb interaction. Extrinsic properties are directly related to dopants, which usually create electronic states in the band gap, and hence influence both optical absorption and emission processes [7].

In our work, we will investigate the complex refractive index i.e. the refractive index and the extinction coefficient via the correlation between m-lines and UV-Vis spectroscopy of Co doped ZnO thin films elaborated by spray pyrolysis.

2 Experimental

The sprayed solution for the undoped ZnO thin films was prepared by dissolving dihydrate zinc acetate [$\mathrm{Zn(CH3CO2)2{\cdot}2H_2O}$] in 99.98% pure methanol to obtain 0.1 M solution that went a constant stirring at 60 °C for 45 minutes on a magnetic stirrer. The sprayed solutions of the Co doped ZnO thin films were prepared under the same conditions and by using cobalt acetate [$\mathrm{Co(CH3CO2)2{\cdot}4H_2O}$] as a Co precursor. Each time the proper amount was added to 0.1 M [$\mathrm{Zn(CH3CO2)2 \cdot 2H_2O}$] dissolved in methanol to produce the following contents of zinc and cobalt: $\mathrm{Co_xZn_{1-x}O}$ with x equals 0.04, 0.08 and 0.10, in addition the reference thin film where x=0.
Ordinary glass substrates were ultra-sonically cleaned in a 1:1 mixture of acetone and ethanol for 15 minutes and left to dry in air. The films were deposited using spray pyrolysis at a deposition temperature of 450 °C.
In order to characterize our thin films, multiple techniques were used: Horiba Jobin Yvon HR800 instrument at excitation wavelength of 473 nm for micro Raman investigation. Scanning electron microscope JEOL JSM-7001F model for morphology purposes. Finally for the optical measurements, Metricon 2010/M Prism (rutile TiO2: n_e=2.8639 and n_o=2.5822 at 632.8 nm with an apical angle of 44,60 °) Coupler was used to couple 632.8 nm He-Ne laser light into air/$\mathrm{Co_xZn_{1-x}O}$/glass waveguide and Shimadzu UV-3101PC UV-Vis-NIR Scanning Spectrophotometer with wavelength range of 190 - 1100 nm and resolution length range of 0.1 nm.

3 Results and discussion

3.1 Micro Raman spectroscopy

Micro-Raman spectroscopy was used to study the impact of cobalt impurities on the crystal structure of ZnO thin films. This method permitted to detect disorder and defect states due to dopant incorporation. Figure 1 showed the micro-Raman spectra of pure and Co doped ZnO thin films in the range of 70-700 cm^{-1}. The undoped ZnO sample exhibited two clearly Raman-active peaks appeared around 102, 441 cm^{-1} and a very weak hump around 570 cm^{-1}. The peaks at 102 and 440 cm^{-1} were associated with E_2 (low) of non polar vibration for heavier Zn atom and E_2 (high) of oxygen displacement [14–16]. In fact, the weak hump was the result of two overlapped peaks localized at 537 and 577 cm^{-1} and were ascribed to A_1(low)/E_1(low) [17, 18]. Co doped ZnO thin films showed similar peaks of the undoped sample with decrease in intensity of the oxygen displacement peak (E_2 (high)) and the enhancement of the mixed A_1(Low)/E_1(low) peaks. In the work of Liu et al. [19] about ZnO thin films, it had been reported that the mixed A_1(Low)/E_1(low) peaks were due to the crystal imperfection and defects such as zinc interstitials and oxygen vacancies. Also, Ponnusamy et al. [20] reported that these peaks arose possibly because of defects. In any case, the Raman behavior of our thin films can be ascribed to the substituted cobalt anions which provoked structural defects and therefore energetic defects in ZnO lattice.

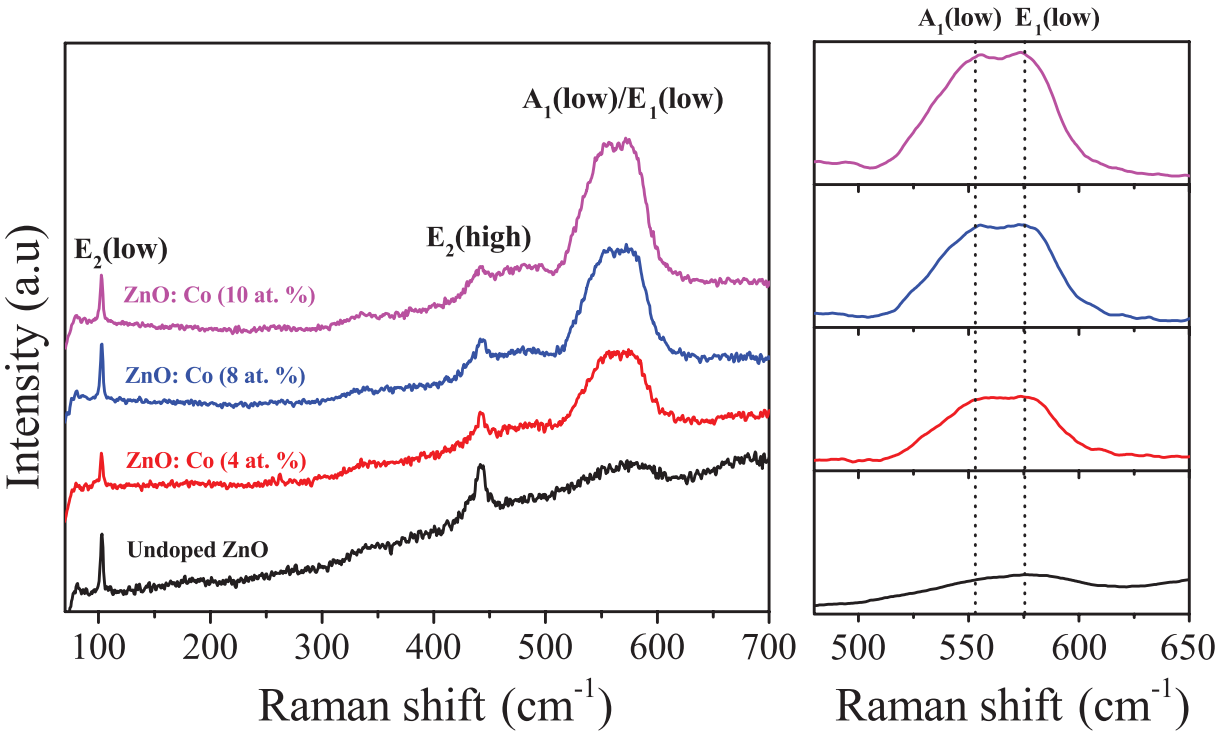

Figure 1: Micro Raman spectra for undoped and Co doped ZnO thin films.

3.2 UV-Vis Measurements

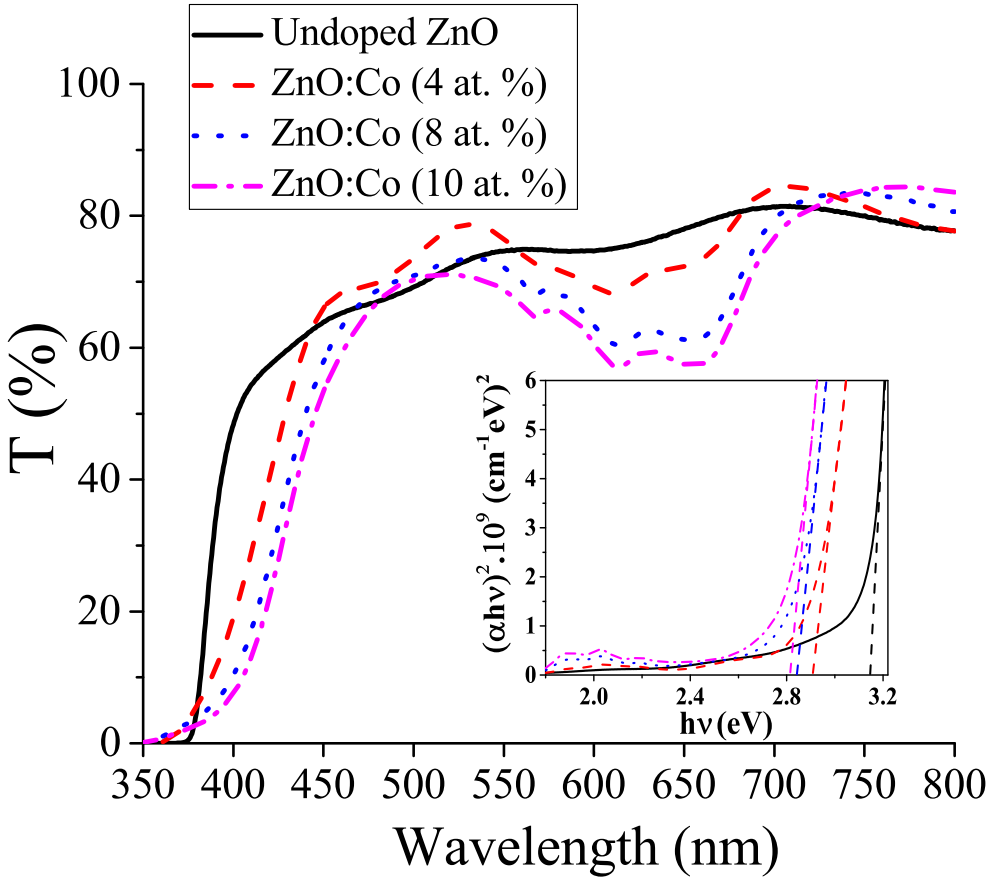

Figure 2: Transmittance spectra and Tauc plot for undoped and Co doped ZnO thin films.

The optical transmission spectra of undoped and Co doped ZnO thin films in the range of 350–800 nm were depicted in figure 2. All films exhibited good optical transmittance. In the region ranging from 500 to 750 nm we can clearly observe a decrease in the average transmittance from 84 to 57 % with the increase of cobalt concentration. The observed spectra were very similar to those obtained in the literature for Co doped ZnO thin films [21–25]. Due to the similar ionic radii of Zn^{+2} (0.60 Å) and Co^{+2} (0.58 Å) [26–28] the substitution of Zn^{+2} by Co^{+2} ions in the tetrahedral coordinated structure was apparent as absorption bands at 568, 613 and 658 nm. These bands were attributed to electronic transitions in $3d$ levels of Co^{+2} (d-d transitions) [29, 30]. Furthermore, the sharp absorption edge experienced a red shift upon Co doping indicating the decrease in the optical band gap. The optical band gap E_g was calculated using the Tauc relation [31]:

$$\alpha h\nu = B(h\nu - E_g)^m \tag{1}$$

where α is the absorption coefficient, $h\nu$ is the photon energy, B is a constant and the exponent m depends on the nature of electronic transition (m = 1/2 for allowed direct transition of ZnO optical band). The optical band gap energy of all films was calculated by linear interpolation of $(\alpha h\nu)^2$ versus $h\nu$ (figure 2). The values decreased from 3.15 to 2.81 eV as Co doping increased from 0 to 10 at. % (figure 3) due to crystal field splitting of Co^{+2} $3d$ levels by the wurtzite structure. These new electronic states give rise to new donor electronic states just below the conduction band, in other words, the decrease in the optical band gap was the result to exchange interactions between the localized d state of Co^{+2} and the s-p state of the ZnO conduction band [32–36].

The Urbach energy is a characteristic parameter of energetic disorder in the band edges. It was calculated based on the next equation [37]:

$$\ln(\alpha) = \ln(\alpha_0) + \frac{h\nu}{E_U} \tag{2}$$

where α_0 is a constant, $h\nu$ is the photon energy and E_U is the Urbach energy. Figure 3 depicted the evolution of the Urbach energy as a function of Co at. % dopant. It had been found to increase over Co content. This was a positive indication for the increase in the energetic disorder present in the films which is directly related to structural defects. This was in good correlation with the increase in the intensity of A_1(low)/E_1(low) peaks as a function of Co doping according to Raman spectra.

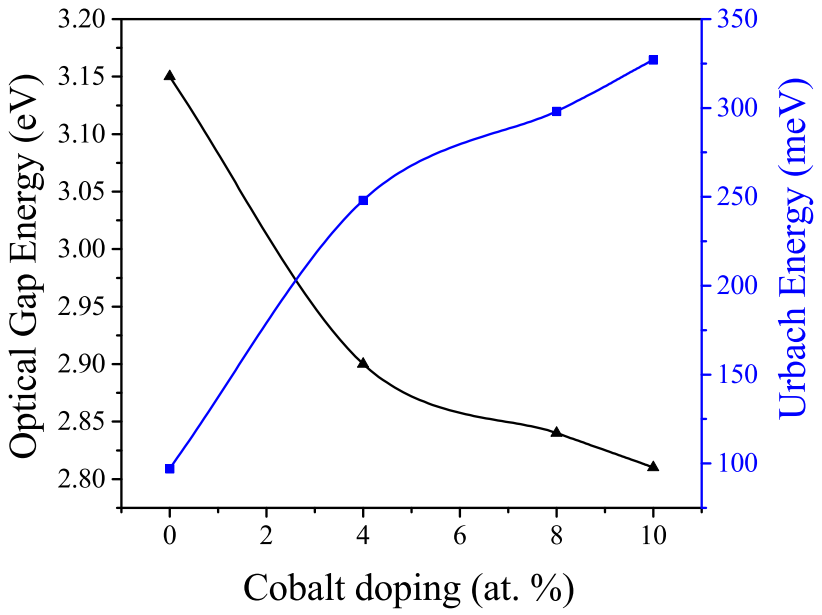

Figure 3: The evolution of both the optical gap energy (E_g) and the Urbach energy (E_U) as a function of Co doping.

3.3 SEM observation

SEM images and the grains size distribution of undoped and 8 at. % Co doped ZnO thin films were shown in figures 4. The undoped film showed grains of a mean diameter of around 280 nm formed by many crystallite aggregates with few pores surrounding them. For the 8 at.% Co doped sample, it showed a dense bi-modal structure with bigger plated grains of a mean diameter close to 200 nm and finer plated grains with a mean diameter in the vicinity of 130 nm. Similar observations were reported by Salah et al. [38] for sprayed pyrolysis Co doped ZnO thin films. In any case, the homogeneity across large-scale makes our thin films suitable for waveguiding applications.

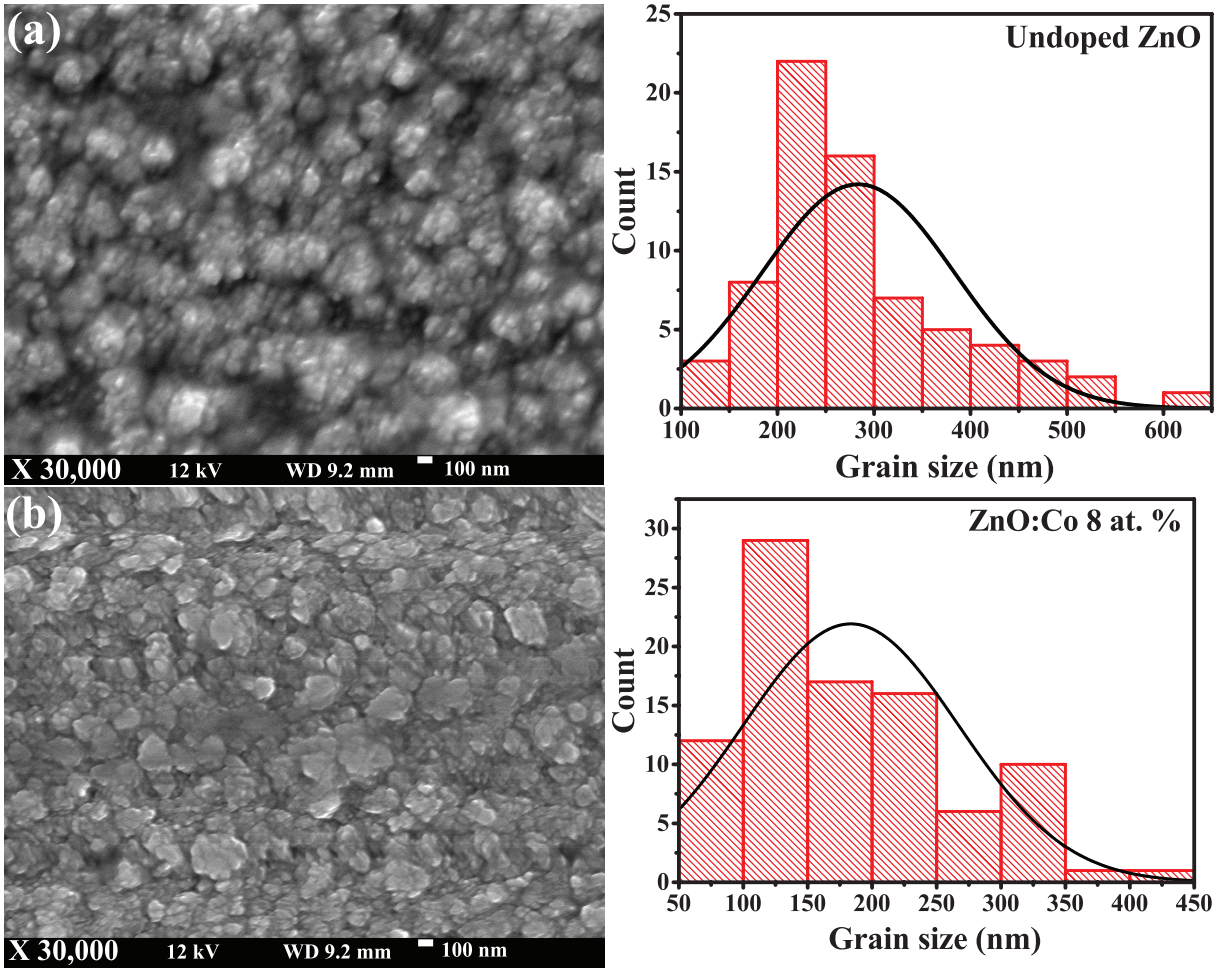

Figure 4: SEM images and grain size distribution of (a) undoped and (b) 8 at. % Co doped ZnO thin films.

3.4 M-lines measurements

In order to understand the effect of Co doping on the waveguiding properties of ZnO thin films, we used prism coupler technique to measure the thickness and the ordinary refractive index in the

Transverse Electric (TE) polarization. The dispersion curves for the TE polarization was given by the following equation:

$$k_0 d\sqrt{n^2 - n_{eff}^2} = \arctan\left(\sqrt{\frac{n_{eff}^2 - n_a^2}{n^2 - n_{eff}^2}}\right) + \arctan\left(\sqrt{\frac{n_{eff}^2 - n_s^2}{n^2 - n_{eff}^2}}\right) + m\pi \tag{3}$$

where n, n_a and n_s are the refraction indexes of the film, superstrate, substrate respectively. m is the mode number. n_{eff} is the effective index of the mode m and $k_0 = \frac{2\pi}{\lambda}$ is the wavevector in vacuum. For at least two propagation modes ($m = 0$ and $m = 1$) [39], we can calculate the refractive index and the thickness by simultaneously solving the resulting equations [40].

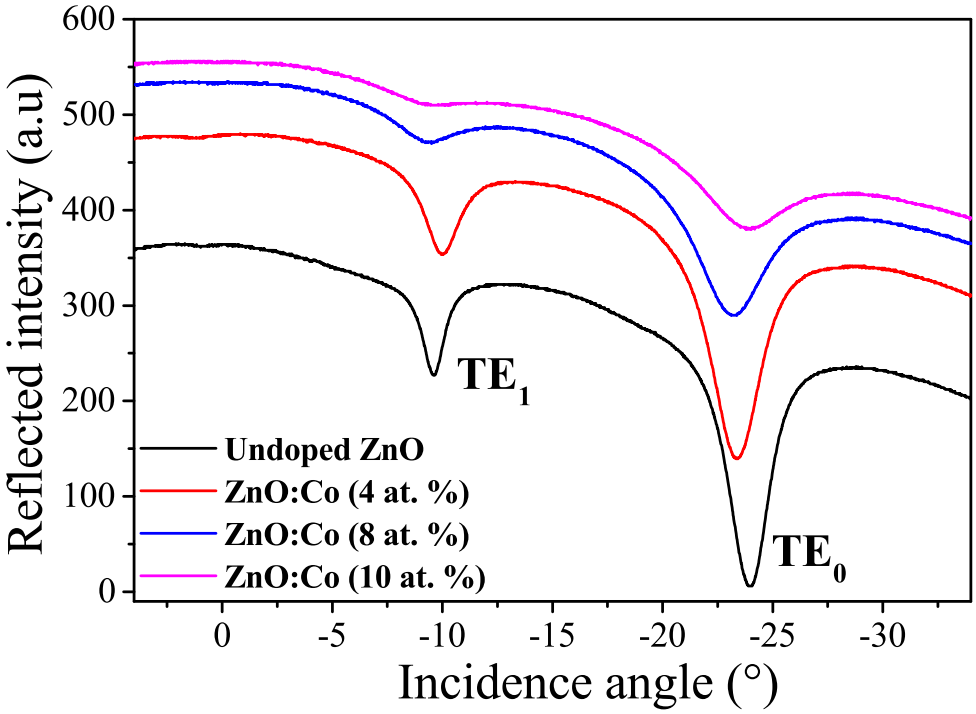

Figure 5: The reflected intensity of the transverse electric (TM) polarization for two waveguide modes as a function of the incidence angle for undoped and Co doped ZnO thin films.

For a plane wave traveling inside a lossy media in the form of a slob waveguide in the z direction, $\phi = \phi_0 \exp(-\gamma z + iwt)$, the propagation constant of the mode m is of the form [41]:

$$\gamma_m = \alpha + i\beta_m \tag{4}$$

where α is the absorption coefficient, β is the phase constant and they are given by:

$$\alpha = 2k_0 \cdot k; \quad \beta_m = k_0 \cdot n_{eff} \tag{5}$$

where k is the extinction coefficient.

The extinction coefficient k was evaluated using UV-Vis measurement as it is directly related to the absorption coefficient and can be calculated using the transmittance T and the thickness d of the films as indicated in the following relation [42]:

$$\alpha = \frac{\ln\left(\frac{1}{T}\right)}{d} \tag{6}$$

The effective index was evaluated by m-lines spectroscopy using the Snell-Decartes equation of refraction [43]:

$$n_{eff} = n_p \sin\left(\arcsin\left(\frac{n_a \sin(\theta)}{n_p}\right) + \theta_p\right) \tag{7}$$

where n_p,n_a and θ_p are the refractive index of the prism, the superstrate and the base angle of the prism respectively. By varying the incident angle on the prism's side θ, we can excite many modes.

Figure 5 presented the reflected intensity vs. the incident angle in the TE polarization. All films experienced two guiding modes. The curves exhibited extinction behavior with Co doping through the diminishing intensity and broadening of the peaks indicating the degradation of the light coupling and propagation in an in the films.

In order to explain the behavior of the refractive index with the optical band gap evolution, we adopted the single oscillator approximation [44, 45]. The refractive index as a function the energy of the incoming light E is of the following:

$$n^2 = \frac{E_o E_d}{E_o^2 - E^2} + 1 \tag{8}$$

where E_d is a measure of the strength of inter-band optical transitions, E_o is the single-oscillator energy. According to Wemple–DiDomenico model, the single-oscillator energy can be approximated in terms of the optical gap energy as: $E_g \approx \frac{E_o}{2}$. The value of E_d for Zn^{+2} is close to that of Co^{+2} [46] and it was supposed to be unchanged.

The ordinary refractive index, the extinction coefficient and the Full Width at Half Maxima (FWHM) of the m-lines peaks were plotted in figure 6. The ordinary refractive index experienced

a slight increase upon cobalt content. In fact, the introduction of Co into ZnO had a decreasing effect on the optical gap which increased the refractive index according to the previous equation of the single oscillator approximation. The decrease in the optical gap energy lowered the energy for electrons to be able to oscillate and contribute to the phase difference measured as an increase in the refractive index [6, 47]. In other words, the electronic polarizability which originates from the electronic cloud deformation was facilitated by the decrease in the optical gap energy. The extinction coefficient had a similar behavior. The introduction of Co in the films rendered the films to be more absorbent at 632.8 nm due to Co^{+2} d-d transitions in the visible region as previously discussed in the UV-Vis section. The light coupling propagation in the films was therefore less efficient since the ZnO thin films passed from dielectric state suitable for waveguiding to more absorbent state not very suitable. This effect was confirmed by broadening of the width and diminishing in intensity of m-lines peaks with their angular position remained virtually the same [13, 48].

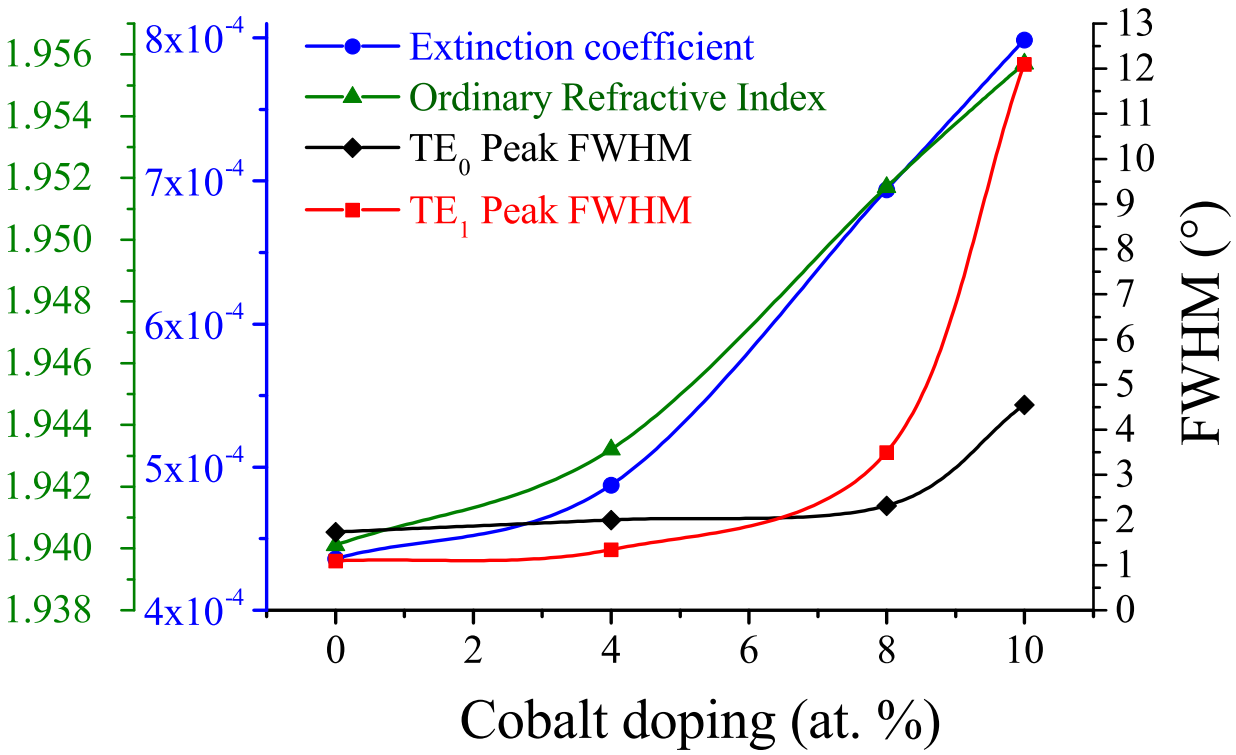

Figure 6: Ordinary refractive index, extinction coefficient, full with at half maximum of the TE_0 and TE_1 peaks over Co at. % doping.

Conclusion

In this work we had reported the successful deposition of Co doped ZnO thin films by spray pyrolysis. All films had a wurtzite structure according to micro Raman spectroscopy.. A decrease in the intensity of oxygen displacement peak (E_2 (high)) and an increase in intensity of structural defects peaks (A_1(Low)/E_1(low)) were observed over Co doping . According to UV-Vis measurements, the introduction of Co in ZnO had also induced the creation of new intrinsic and extrinsic electronic states. Optical band gap was found to decrease with Co doping due to external sp-d transitions. The energetical defects evolution had been confirmed by the Urbach energy calculation. M-lines spectroscopy allowed for the measurements of the ordinary refractive index and it increased as the Co doping increased which was attributed to the decrease in the gap energy based on the single oscillator approximation. Furthermore, ZnO thin films developed absorbing behavior with Co which was obvious in the increase in both the full width at half maximum of the guiding peaks and the extinction coefficient in addition to the decrease in the reflected intensity. This was related to internal d-d transitions which affected light coupling and propagation.
The correlation between m-lines and UV-Vis measurements seems to be very reliable method to measure the complex refractive index of relatively high refractive index transparent waveguide. It is simple and inexpensive in comparison to other optical techniques.

Competing Interests

There are no conflicts of interest between the authors.

Author Contribution

Y. Bouachiba conceived the idea of the articles and m-lines measurements. The elaboration of the films in addition to UV-Vis and micro-Raman measurements were carried out by H. Djaaboube. scanning electron microscope images were performed by I.Sekhri. All others contributed to the interpretation of the results and provided critical feedback and helped shape the research, analysis and manuscript.

Research Data Policy and Data Availability Statements

The datasets generated during and/or analysed during the current study are included in the manuscript and available from the corresponding author on reasonable request.

References

[1] Jenq-Nan Yih, Yi-Ming Chu, Yen-Chieh Mao, Wei-Han Wang, Fan-Ching Chien, Chun-Yu Lin, Kuang-Li Lee, Pei-Kuen Wei, and Shean-Jen Chen. Optical waveguide biosensors constructed with subwavelength gratings. *Appl. Opt.*, 45(9):1938–1942, Mar 2006.

[2] Francesco Arcadio, Luigi Zeni, Aldo Minardo, Caterina Eramo, Stefania Ronza, Chiara Perri, Girolamo D'Agostino, Guido Chiaretti, Giovanni Porto, and Nunzio Cennamo. A nanoplasmonic-based biosensing approach for wide-range and highly sensitive detection of chemicals. *Nanomaterials*, 11:1961, 07 2021.

[3] Harshini Mukundan, Aaron Anderson, W Grace, Karen Grace, Nile Hartman, Jennifer Martinez, and Basil Swanson. Waveguide-based biosensors for pathogen detection. *Sensors (Basel, Switzerland)*, 9:5783–809, 07 2009.

[4] J. Ben Naceur, M. Gaidi, F. Bousbih, R. Mechiakh, and R. Chtourou. Annealing effects on microstructural and optical properties of Nanostructured-TiO2 thin films prepared by sol–gel technique. *Current Applied Physics*, 12(2):422–428, March 2012.

[5] Anish Priyadarshi, Firehun Tsige Dullo, Deanna Lynn Wolfson, Azeem Ahmad, Nikhil Jayakumar, Vishesh Dubey, Jean-Claude Tinguely, Balpreet Singh Ahluwalia, and Ganapathy Senthil Murugan. A transparent waveguide chip for versatile total internal reflection fluorescence-based microscopy and nanoscopy. *Communications Materials*, 2(1):1–11, 2021.

[6] Richard Phillips Feynman, Robert Benjamin Leighton, and Matthew Sands. *The Feynman lectures on physics; New millennium ed.* Basic Books, New York, NY, 2010. Originally published 1963-1965.

[7] Chennupati Jagadish and Stephen J Pearton. *Zinc oxide bulk, thin films and nanostructures: processing, properties, and applications*. Elsevier, 2011.

[8] W.S. Hu, Z.G. Liu, X.L. Guo, C. Lin, S.N. Zhu, and D. Feng. Preparation of c-axis oriented zno optical waveguiding films on fused silica by pulsed laser reactive ablation. *Materials Letters*, 25(1):5–8, 1995.

[9] N. Mais, J. P. Reithmaier, A. Forchel, M. Kohls, L. Spanhel, and G. Müller. Er doped nanocrystalline zno planar waveguide structures for 1.55 μm amplifier applications. *Applied Physics Letters*, 75(14):2005–2007, 1999.

[10] S. F. Yu, Clement Yuen, S. P. Lau, Y. G. Wang, H. W. Lee, and B. K. Tay. Ultraviolet amplified spontaneous emission from zinc oxide ridge waveguides on silicon substrate. *Applied Physics Letters*, 83(21):4288–4290, 2003.

[11] Navina Mehan, Vinay Gupta, Kondepudy Sreenivas, and Abhai Mansingh. Effect of annealing on refractive indices of radio-frequency magnetron sputtered waveguiding zinc oxide films on glass. *Journal of Applied Physics*, 96(6):3134–3139, 2004.

[12] Julien Cardin and Dominique Leduc. Determination of refractive index, thickness, and the optical losses of thin films from prism-film coupling measurements. *Appl. Opt.*, 47(7):894–900, Mar 2008.

[13] V. Sokolov, N. Marusin, V. Panchenko, Alexander Savelyev, V. Seminogov, and E. Khaydukov. Determination of refractive index, extinction coefficient and thickness of thin films by the method of waveguide mode excitation. *Quantum Electronics*, 43, 11 2013.

[14] T. C. Damen, S. P. S. Porto, and B. Tell. Raman effect in zinc oxide. *Phys. Rev.*, 142:570–574, Feb 1966.

[15] X.F Wang, J.B Xu, B. Zhang, H.G. Yu, J. Wang, X. Zhang, J.G. Yu, and Q. Li. Signature of intrinsic high-temperature ferromagnetism in cobalt-doped zinc oxide nanocrystals. *Advanced Materials*, 18(18):2476–2480, 2006.

[16] J. M. Calleja and Manuel Cardona. Resonant raman scattering in zno. *Phys. Rev. B*, 16:3753–3761, Oct 1977.

[17] Xuefeng Wang, Jianbin Xu, Xiaojiang Yu, Kun Xue, Jiaguo Yu, and Xiujian Zhao. Structural evidence of secondary phase segregation from the raman vibrational modes in zn1-xcoxo (0<x<0.6). *Applied Physics Letters*, 91(3):031908, 2007.

[18] Marcel Schumm. *ZnO-based semiconductors studied by Raman spectroscopy: semimagnetic alloying, doping, and nanostructures*. PhD thesis, Universität Würzburg, 2008.

[19] Yang Li, Wenlan Qiu, Fan Qin, Hui Fang, Viktor G. Hadjiev, Dmitri Litvinov, and Jiming Bao. Identification of cobalt oxides with raman scattering and fourier transform infrared spectroscopy. *The Journal of Physical Chemistry C*, 120(8):4511–4516, 2016.

[20] Rajeswari Ponnusamy, Dhanuskodi Sivasubramanian, P. Sreekanth, Vinitha Gandhiraj, Reji Philip, and G. M. Bhalerao. Nonlinear optical interactions of co: Zno nanoparticles in continuous and pulsed mode of operations. *RSC Adv.*, 5:80756–80765, 2015.

[21] Fereshteh Akhtari, Suzan Zorriasatein, Majid Farahmandjou, and Seyed Mohammad Elahi. Structural, optical, thermoelectrical, and magnetic study of $\mathrm{zn_{1-x}co_xo}$ ($0 \leq x \leq 0.10$) nanocrystals. *International Journal of Applied Ceramic Technology*, 15(3):723–733, 2018.

[22] H. Ndilimabaka, S. Colis, G. Schmerber, D. Müller, J.J. Grob, L. Gravier, C. Jan, E. Beaurepaire, and A. Dinia. As-doping effect on magnetic, optical and transport properties of zn0.9co0.1o diluted magnetic semiconductor. *Chemical Physics Letters*, 421(1):184–188, 2006.

[23] M Naeem, S K Hasanain, and A Mumtaz. Electrical transport and optical studies of ferromagnetic cobalt doped ZnO nanoparticles exhibiting a metal–insulator transition. *Journal of Physics: Condensed Matter*, 20(2):025210, dec 2007.

[24] B. Salameh, A.M. Alsmadi, and M. Shatnawi. Effects of co concentration and annealing on the magnetic properties of co-doped zno films: Role of oxygen vacancies on the ferromagnetic ordering. *Journal of Alloys and Compounds*, 835:155287, 2020.

[25] O. Gençyılmaz, F. Atay, and İ. Akyüz. Photoluminescence, ellipsometric, optical and morphological studies of sprayed co-doped zno films. *Modern Physics Letters B*, 30(15):1650171, 2016.

[26] Robert D Shannon. Revised effective ionic radii and systematic studies of interatomic distances in halides and chalcogenides. *Acta crystallographica section A: crystal physics, diffraction, theoretical and general crystallography*, 32(5):751–767, 1976.

[27] A. S. Risbud, N. A. Spaldin, Z. Q. Chen, S. Stemmer, and Ram Seshadri. Magnetism in polycrystalline cobalt-substituted zinc oxide. *Phys. Rev. B*, 68:205202, Nov 2003.

[28] Hongfen Ji, Changlong Cai, Shun Zhou, and Weiguo Liu. Structure, photoluminescence, and magnetic properties of co-doped zno nanoparticles. *Journal of Materials Science: Materials in Electronics*, 29(15):12917–12926, 2018.

[29] P. Koidl. Optical absorption of $\mathrm{co^{2+}}$ in zno. *Phys. Rev. B*, 15:2493–2499, Mar 1977.

[30] Kwang Joo Kim and Young Ran Park. Spectroscopic ellipsometry study of optical transitions in zn1-xcoxo alloys. *Applied Physics Letters*, 81(8):1420–1422, 2002.

[31] J. Tauc, R. Grigorovici, and A. Vancu. Optical properties and electronic structure of amorphous germanium. *physica status solidi (b)*, 15(2):627–637, 1966.

[32] J. K. Furdyna. Diluted magnetic semiconductors. *Journal of Applied Physics*, 64(4):R29–R64, 1988.

[33] K.T. Ramakrishna Reddy, V. Supriya, Y. Murata, and M. Sugiyama. Effect of co-doping on the properties of zn1-xcoxo films deposited by spray pyrolysis. *Surface and Coatings Technology*, 231:149–152, 2013. Taiwan Association for Coating and Thin Film Technology (TACT 2011).

[34] S. Venkataprasad Bhat and F.L. Deepak. Tuning the bandgap of zno by substitution with mn2+, co2+ and ni2+. *Solid State Communications*, 135(6):345–347, 2005.

[35] Aihua Wang, Binglin Zhang, Xinchang Wang, Ning Yao, Zhifeng Gao, Yukun Ma, Lan Zhang, and Huizhong Ma. Nano-structure, magnetic and optical properties of co-doped ZnO films prepared by a wet chemical method. *Journal of Physics D: Applied Physics*, 41(21):215308, oct 2008.

[36] Z Aghagoli and M Ardyanian. Synthesis and study of the structure, magnetic, optical and methane gas sensing properties of cobalt doped zinc oxide microstructures. *Journal of Materials Science: Materials in Electronics*, 29(9):7130–7141, 2018.

[37] Biswajit Choudhury, Munmun Dey, and Amarjyoti Choudhury. Defect generation, d-d transition, and band gap reduction in cu-doped tio2 nanoparticles. *International Nano Letters*, 3, 04 2013.

[38] Abeer Salah, Ahmed M. Saad, and Ahmed A. Aboud. Effect of co-doping level on physical properties of zno thin films. *Optical Materials*, 113:110812, 2021.

[39] B. Gharbi, Adel Taabouche, M. Brella, Rachid Gheriani, Y. Bouachiba, Abderrahmane Bouabellou, Faouzi Hanini, Samuel Louis Barouk, Houda Serrar, and Badis Rahal. Spray pyrolysis synthesized and zno–nio nanostructured thin films analysis with their nanocomposites for waveguiding applications. *Semiconductors*, 55:37–43, 2021.

[40] R. Ulrich and R. Torge. Measurement of thin film parameters with a prism coupler. *Appl. Opt.*, 12(12):2901–2908, Dec 1973.

[41] Irwin J Kurland and Henry L Bertoni. Birefringent prism couplers for thin-film optical waveguides. *Applied optics*, 17(7):1030–1037, 1978.

[42] Jiawei Gong and Sumathy Krishnan. Chapter 2 - mathematical modeling of dye-sensitized solar cells. In Masoud Soroush and Kenneth K.S. Lau, editors, *Dye-Sensitized Solar Cells*, pages 51–81. Academic Press, 2019.

[43] Y. Bouachiba, A. Taabouche, A. Bouabellou, F. Hanini, C. Sedrati, and H. Merabti. TiO_2 waveguides thin films prepared by sol-gel method on glass substrates with and without ZnO underlayer. *Materials Science-Poland*, 38(3):381–385, September 2020.

[44] R. Orainy. Single oscillator model and refractive index dispersion properties of ternary zno films by sol gel method. *Journal of Sol-Gel Science and Technology*, 70, 04 2014.

[45] F. Yakuphanoglu, A. Cukurovali, and İ. Yilmaz. Single-oscillator model and determination of optical constants of some optical thin film materials. *Physica B: Condensed Matter*, 353(3):210–216, 2004.

[46] Xiao-Yong Gao, Hong-Liang Feng, Jiao-Min Ma, Zeng-Yuan Zhang, Jing-Xiao Lu, Yong-Sheng Chen, Shi-E Yang, and Jin-Hua Gu. Analysis of the dielectric constants of the ag2o film by spectroscopic ellipsometry and single-oscillator model. *Physica B: Condensed Matter*, 405(7):1922–1926, 2010.

[47] Kamal A Aly. Optical band gap and refractive index dispersion parameters of as x se 70 te 30-x ($0 \leq x \leq 30$ at.%) amorphous films. *Applied Physics A*, 99(4):913–919, 2010.

[48] Takayuki Okamoto, Mari Yamamoto, and Ichirou Yamaguchi. Optical waveguide absorption sensor using a single coupling prism. *J. Opt. Soc. Am. A*, 17(10):1880–1886, Oct 2000.